

ORIGINAL PAPERS

Human and mouse mesotheliomas exhibit elevated AKT/PKB activity, which can be targeted pharmacologically to inhibit tumor cell growth

Deborah A Altomare¹, Huihong You¹, Guang-Hui Xiao¹, Maria E Ramos-Nino², Kristine L Skele¹, Assunta De Rienzo¹, Suresh C Jhanwar³, Brooke T Mossman², Agnes B Kane⁴ and Joseph R Testa^{*1}

¹Human Genetics Program, Fox Chase Cancer Center, 333 Cottman Avenue, Philadelphia, PA 19111, USA; ²Department of Pathology, University of Vermont College of Medicine, 89 Beumont Avenue, Burlington, VT 05405, USA; ³Department of Medicine, Memorial Sloan-Kettering Cancer Center, 1275 York Avenue, New York, NY 10021, USA; ⁴Department of Pathology and Laboratory Medicine, Brown University, 70 Ship Street, Providence, RI 02912, USA

Malignant mesotheliomas (MMs) are very aggressive tumors that respond poorly to standard chemotherapeutic approaches. The phosphatidylinositol 3-kinase (PI3K)/AKT pathway has been implicated in tumor aggressiveness, in part by mediating cell survival and reducing sensitivity to chemotherapy. Using antibodies recognizing the phosphorylated/activated form of AKT kinases, we observed elevated phospho-AKT staining in 17 of 26 (65%) human MM specimens. In addition, AKT phosphorylation was consistently observed in MMs arising in asbestos-treated mice and in MM cell xenografts. Consistent with reports implicating hepatocyte growth factor (HGF)/Met receptor signaling in MM, all 14 human and murine MM cell lines had HGF-inducible AKT activity. One of nine human MM cell lines had elevated AKT activity under serum-starvation conditions, which was associated with a homozygous deletion of *PTEN*, the first reported in MM. Treatment of this cell line with the mTOR inhibitor rapamycin resulted in growth arrest in G1 phase. Treatment of MM cells with the PI3K inhibitor LY294002 in combination with cisplatin had greater efficacy in inhibiting cell proliferation and inducing apoptosis than either agent alone. Collectively, these data indicate that MMs frequently express elevated AKT activity, which may be targeted pharmacologically to enhance chemotherapeutic efficacy. These findings also suggest that mouse models of MM may be useful for future preclinical studies of pharmaceuticals targeting the PI3K/AKT pathway.

Oncogene (2005) 24, 6080–6089. doi:10.1038/sj.onc.1208744; published online 16 May 2005

Keywords: AKT; mTOR; asbestos; mesothelioma

Introduction

Malignant mesotheliomas (MMs) are aggressive neoplasms that arise primarily from the surface serosal cells of the pleural, peritoneal, and pericardial cavities. Epidemiological studies have established that exposure to asbestos fibers is the primary cause of MM (Craighead and Mossman, 1982). Even with widespread asbestos abatement efforts, the incidence of MM may increase in Western Europe and the United States until approximately 2020, and since the development of MM is associated with a 20–40 year latency from the time of asbestos exposure, the unregulated use of asbestos in less industrialized countries may prolong the epidemic in those regions (Britton, 2002).

The pathogenesis and tumor biology of MM is incompletely understood because diagnosis is usually made late in tumor progression. Generally, response rates to either single-agent or combination chemotherapy have not surpassed 20%, with median survivals of approximately 6–8 months (Rusch, 2003), although increased enthusiasm for multimodality treatment may be spurred by the results of a recent phase II trial showing a 40% response rate among MM patients receiving pemetrexed combined with cisplatin (Vogelzang *et al.*, 2003). Novel agents under study in phase II trials of MM patients include ZD1839 (Iressa) and ST1-571 (Gleevec), highly selective inhibitors of the epidermal growth factor receptor (EGFR) and platelet-derived growth factor (PDGF) and c-Kit receptors, respectively (Nowak *et al.*, 2002). Thus, there is rationale for improved therapeutic approaches, perhaps with the use of new low-toxicity pharmaceuticals that target signal transduction cascades important for MM tumor cell growth and proliferation.

A growing body of evidence suggests that AKT perturbations play an important role in human cancer, and numerous AKT substrates have been implicated in tumorigenesis (Bellacosa *et al.*, in press). Activation of AKT triggers antiapoptotic mechanisms, positively influences NF- κ B transcription, modulates angiogenesis, enhances telomerase activity, increases tumor invasion/metastasis, and antagonizes cell cycle arrest. AKT also

*Correspondence: JR Testa; E-mail: jr_testa@fccc.edu
Received 5 November 2004; revised 29 March 2005; accepted 29 March 2005; published online 16 May 2005

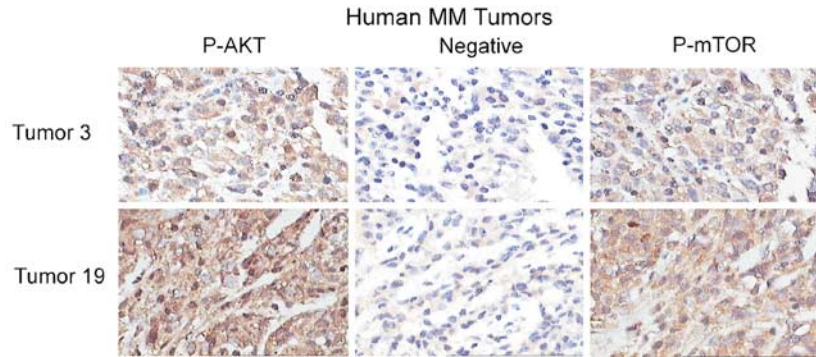


Figure 1 AKT is frequently activated in human MM tumors and is associated with phosphorylation of mTOR. Immunohistochemical staining of representative MM tumors from a tissue microarray showing the absence of staining in a negative control (blocking peptide for phospho-AKT), and strong positivity (brown stain) for phospho-AKT (P-AKT) and phospho-mTOR (P-mTOR)

mediates mRNA translation by means of phosphorylation of mTOR (mammalian target of rapamycin) protein kinase. Activation of mTOR subsequently leads to the phosphorylation of eukaryotic initiation factor 4E (eIF4E)-binding protein-1 (4E-BP1), thereby dissociating 4E-BP1 from the mRNA cap binding protein eIF4E to promote protein synthesis (Sonenberg and Gingras, 1998). mTOR also regulates the activity of the ribosomal protein S6 kinase (p70S6K), which is required for cell growth and G1 cell cycle progression (Pullen and Thomas, 1997). Currently, targeted disruption of mTOR signaling by rapamycin or its pharmaceutical analogs, CCI-779 (Wyeth) and RAD001 (Novartis), is being tested for efficacy against a broad range of refractory tumors.

To date, the involvement of AKT signaling in MM has not been described. In this investigation, we demonstrate that the AKT pathway is frequently activated in both human and mouse MMs, and that selective pharmacologic targeting of this pathway inhibits MM cell growth and increases sensitivity to conventional chemotherapeutic agents.

Results

Human MM specimens frequently exhibit elevated AKT activity

To determine if AKT is activated in primary human MM specimens, we performed an immunohistochemical analysis using a tumor microarray consisting of 26 paraffin-embedded MM tumor sections using an antibody against phosphorylated Ser473 of AKT, which recognizes the active (phosphorylated) forms of all three AKT kinases in MM specimens. Immunostaining for phospho-AKT was found predominantly in the cytoplasm or at the cell membrane of malignant cells. Overall, 17 of 26 (65%) MM specimens displayed strong staining (+ + or + + +) for phospho-AKT, indicative of elevated levels of AKT activity (Figure 1). As expected, staining was not observed when the antibody was preincubated with a blocking peptide against the phospho-AKT epitope.

Table 1 Immunohistochemical staining for phospho-AKT (P-AKT) is associated with that of phospho-mTOR (P-mTOR)

	<i>Strong P-AKT staining</i>	<i>Weak P-AKT staining</i>
Strong P-mTOR staining	15	0
Weak P-mTOR staining	2	9

To confirm activation of the phosphatidylinositol 3-kinase (PI3K)/AKT pathway, we used an antibody directed at phosphorylated Ser2448 of mTOR to recognize the active form of the downstream mTOR kinase in this same series of MM specimens (Figure 1). No staining was detected when the antibody was preincubated with a blocking peptide against the phospho-mTOR epitope (data not shown). Overall, phospho-mTOR immunostaining was similar to that of phospho-AKT in 24 of 26 (92%) cases, with 15 of 26 (58%) tumors displaying both strong phospho-mTOR and phospho-AKT staining, and nine of 26 (34%) tumors displaying neither AKT nor mTOR staining (Table 1). Statistical analysis of the immunohistochemical staining revealed that phospho-mTOR positivity is significantly associated with that of phospho-AKT (Fisher's exact test, $P < 0.0001$).

Elevated Akt activity in in vivo MM models

We also performed immunohistochemical studies of AKT activity in three *in vivo* models: MMs arising in asbestos-treated mice, MMs arising in a xenograft model of a murine MM cell line, 40L, derived from an asbestos-exposed mouse, and MMs arising in a xenograft model of the human REN cell line derived from a patient with pleural MM (Cao *et al.*, 2001) (Figure 2). Strong phospho-Akt staining was observed in MM tumor nodules located in the peritoneal wall of mice injected intraperitoneally with crocidolite asbestos. Strong phospho-AKT staining was also evident in lung metastases of 40L cells and in tumors arising from the transplantation of REN human MM cells. Like most human MM tumors with strong phospho-AKT staining,

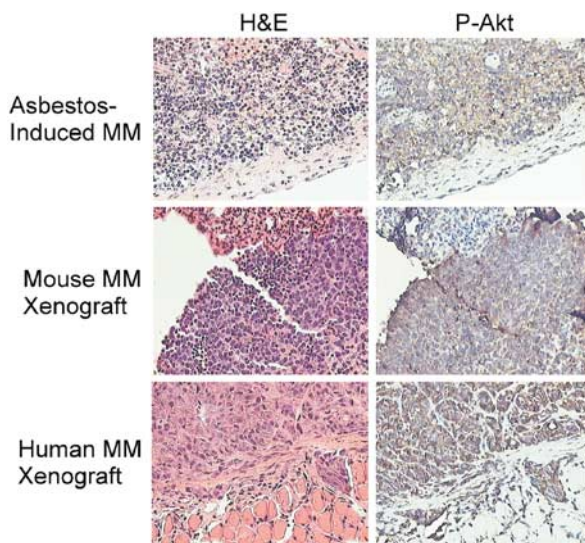


Figure 2 *In vivo* models of MM exhibit activation of AKT. Hematoxylin and eosin-stained sections (left panels) and phospho-AKT immunostaining (right panels) of representative MM tumors from asbestos-treated mice, lung metastasis from a transplanted mouse MM cell line and invasive xenograft established from REN human MM cells. Note the lack of phospho-AKT immunostaining in surrounding stroma, in contrast to the abundant staining in tumor

all of these mouse models of MM exhibited elevated phospho-mTOR (data not shown), thereby confirming the activation of the Akt signaling pathway and the potential utility of these mouse models for future preclinical studies.

Akt/AKT activity is induced in mouse and human MM cells through growth factor stimulation

In vitro studies of MM cell lines may elucidate signaling pathways important for MM tumorigenesis and are useful to identify pharmaceutical agents with potential efficacy in inhibiting MM cell growth. We initially examined five MM cell lines derived from the ascites or intraperitoneal lavage of asbestos-treated mice exhibiting strong phospho-Akt immunostaining, as represented in Figure 2 (top right panel). Overnight serum starvation diminished phospho-Akt levels in this panel of mouse MM cell lines as a result of the lack of growth-factor stimulation, although basal levels of phospho-Akt were still detectable (Figure 3a). Consistent with previous reports suggesting that hepatocyte growth factor (HGF)/Met receptor signaling plays a significant role in MM tumors and cell lines (Tolnay *et al.*, 1998; Harvey *et al.*, 2000) markedly increased phospho-Akt levels were observed in all five murine cell lines stimulated with HGF. In contrast, only one of five mouse MM cell lines exhibited elevated phospho-Akt levels in response to insulin-like growth factor-1 (IGF-1) stimulation.

We next examined the effectiveness of HGF in stimulating AKT activity in human MM cells. Initial studies showed that the Met receptor is strongly

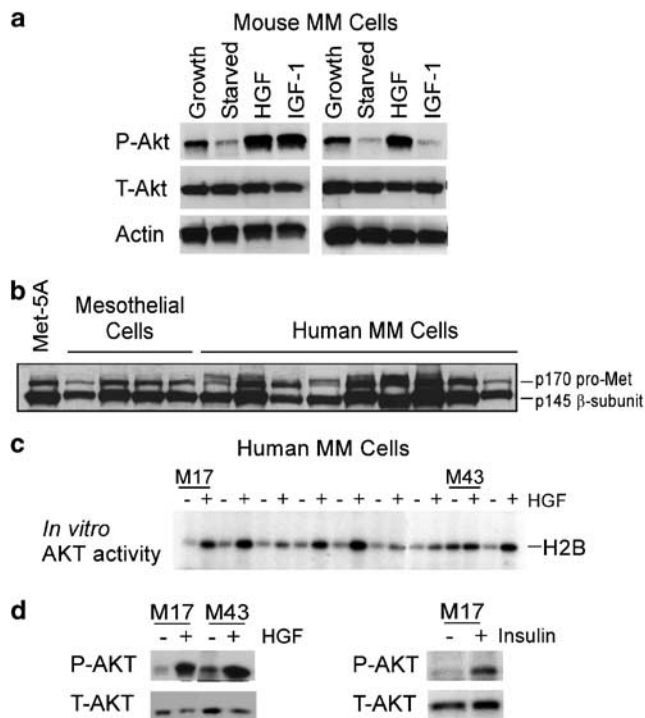


Figure 3 AKT is frequently activated by HGF/growth factor stimulation. (a) Representative Western blots with antibodies against phospho-AKT (P-AKT), total AKT (T-AKT) and actin. All of five MM cell lines from asbestos-treated mice showed HGF-inducible activation of AKT. One of five cell lines (right panel) also exhibited strong IGF-1 activation of AKT. (b) Western blot showing strong Met expression in Met5A immortalized human mesothelial cells, human mesothelial, and MM cell lines. Compared to normal mesothelial cells, Met is overexpressed in five of nine MM cell lines. (c) *In vitro* AKT kinase assay showing HGF stimulation of AKT activity in human MM cell lines, as detected by the *in vitro* phosphorylation of histone H2B. MM cell lines were serum starved overnight (–) and then stimulated with HGF (+) for 10–20 min. Note that only one cell line (M43) exhibited elevated AKT activity under both conditions. A second cell line (M17) had lower basal AKT activity that was inducible by HGF, which was representative of other MM cell lines in this panel. (d) Right, Western blot confirming that HGF stimulates the phosphorylation of AKT in human MM cell lines. Left, representative Western blot showing that other growth factors besides HGF, such as insulin, are able to stimulate AKT activity in human MM cells

expressed in a panel of nine human MM cells, with five of nine cell lines exhibiting overexpression of Met compared to normal mesothelial cells (Figure 3b). Similar to mouse MM cell lines, phospho-AKT levels were detectable under serum-starvation conditions, but were elevated in response to HGF stimulation (Figure 3c). *In vitro* kinase assays originally were used to examine different isoforms of AKT, namely AKT1 and AKT2, with similar results. A Western blot confirmed that HGF stimulates a large increase in AKT activity in two representative human MM cells, including M43 cells with an elevated basal level of AKT activity (Figure 3d, left). Strongly elevated HGF-stimulated AKT activity as detected by Ser473 phospho-specific antibodies may be attributed in part to the antibody's ability to recognize multiple AKT isoforms

simultaneously. In addition, we acknowledge that other growth factors can stimulate AKT activity in MM cells. For example, a representative Western blot depicted in Figure 3d (right) showed that insulin can increase AKT activity in M17 cells. IGF-1, PDGF and EGF also stimulated AKT activity in M17 cells (data not shown).

Elevated AKT activity in a human MM cell line exhibiting loss of PTEN

Interestingly, Tumor 19 in Figure 1 with strong phospho-AKT immunostaining showed elevated Met receptor staining (Figure 4a). In contrast, Tumor 3 had detectable Met expression, but exhibited loss of PTEN staining. Therefore, loss or downregulation of PTEN may be another mechanism contributing to high AKT activity in a subset of MMs.

The elevated basal AKT activity in M43 cells also was found to be associated with a homologous deletion of the *PTEN* tumor suppressor gene (Figure 4b and c).

PTEN exons 2–8 were analysed and found to be absent in M43 cells, based on a single-strand conformation polymorphism (SSCP) assay using primer pairs specific for the coding region of the *PTEN* gene (Figure 4b). PCR analysis of genomic DNA from M43 cells confirmed the loss of exons 2 and 3, using primers that were the same or different from the SSCP analysis (Figure 4c). Primers for GAPDH and exon 1 of *PTEN* amplified bands of the predicted mobility in both M43 cells and control M17 cells, previously shown in Figure 3 to have lower basal AKT activity. M43 cells also exhibited loss of *PTEN* protein, whereas normal mesothelial cells and M17 cells retained *PTEN* protein (Figure 4d).

MM cells with elevated AKT activity are sensitive to inhibition of the PI3K/AKT/mTOR pathway

Various studies have demonstrated that growth of tumor cells with elevated AKT activity is highly sensitive

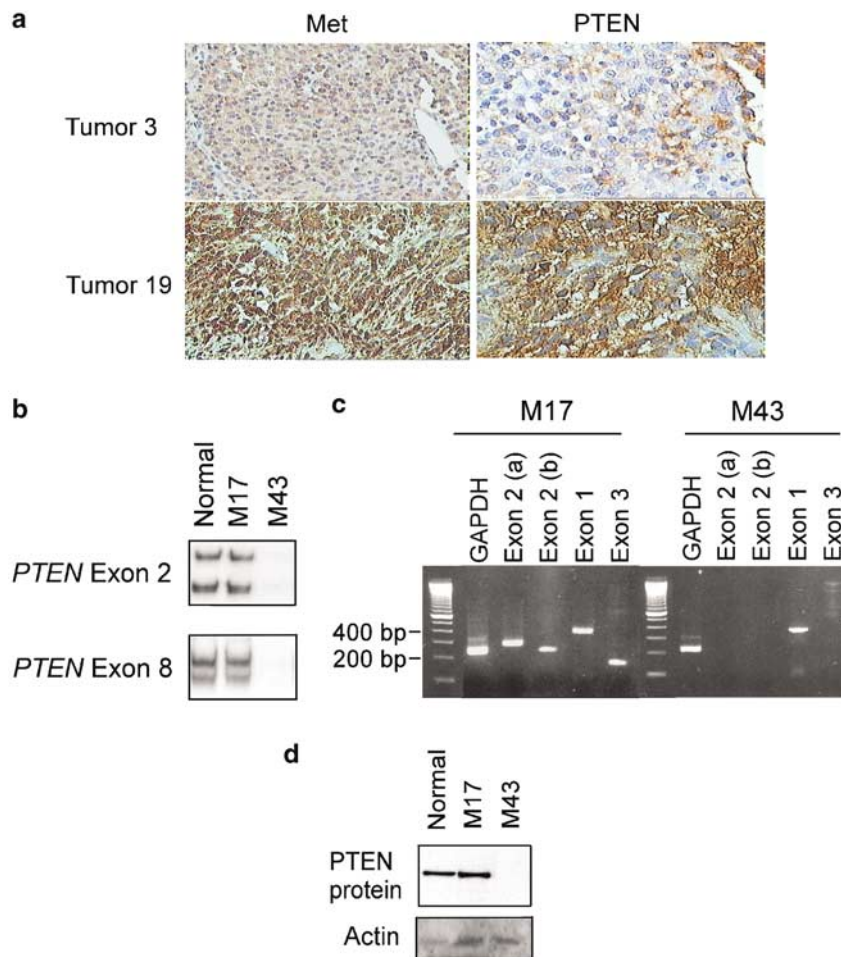


Figure 4 Loss of *PTEN* may contribute to the activation of AKT in MM. (a) Immunohistochemical staining of MM tumors (Figure 1) showing representative overexpression of Met (Tumor 19, left) or loss of *PTEN* protein (Tumor 3, right), which may contribute to the activation of AKT/mTOR in MM tumors. (b) Representative SSCP analysis under denaturing gel electrophoresis conditions showing loss of *PTEN* exons 2 and 8 in M43 cells. (c) PCR analysis of M17 and M43 cells confirming the loss of *PTEN* exons in M43. Primers corresponded to control GAPDH, and *PTEN* exons 1, 2, or 3. PCR reactions for exon 2 used two independent primer pairs (a) or (b) to confirm the absence of signal by SSCP. (d) Immunoprecipitation/Western blot showing the presence of *PTEN* protein in normal mesothelial cells (Normal) and M17 cells, but not in M43 cells

to targeted disruption of AKT signaling (reviewed in Bellacosa *et al.*, in press). Moreover, it has been shown that AKT activity is important for predicting which tumors will be sensitive to mTOR inhibition (Neshat *et al.*, 2001; Podsypanina *et al.*, 2001).

We analysed M43 cells, which have elevated AKT activity, for potential sensitivity to LY294002 and rapamycin, inhibitors of upstream PI3K and downstream mTOR, respectively. As expected, treatment of M43 cells for 48 h with LY294002, but not rapamycin, decreased AKT phosphorylation compared to cells treated with placebo (DMSO) (Figure 5a). Treatment of M43 cells with either inhibitor abolished mTOR activity, as demonstrated by markedly decreased phosphorylation of the downstream p70S6K (Thr389) and S6 ribosomal protein (Ser240/244) (Figure 5a). The cyclin-dependent kinase inhibitor p27^{Kip1}, which is known to be downstream of AKT signaling (reviewed in Wu *et al.*, 2003), was low in M43 cells, but was upregulated in response to LY294002 or rapamycin treatment.

As a follow-up to these studies, cell cycle analyses of M43 cells treated for 48 h with 100 ng/ml rapamycin showed a ~30% increase in the G1 cell population compared to cells treated with placebo (Fisher's exact test, $P=0.016$) (Figure 5b). Thus, MM cells with a dependence on AKT/mTOR signaling exhibit sensitivity to G1 arrest induced by rapamycin. An increase in the sub-G1 population, indicative of increased apoptosis, was not a primary effect of rapamycin in this cell line under the conditions of our study. In contrast, disruption of upstream AKT signaling through the use of the PI3K inhibitor LY294002 affected cell survival, as evidenced by a 3.3-fold increase in the sub-G1 cell population in M43 cells treated for 48 h with 20 μ M LY294002 compared to placebo-treated M43 cells ($P=0.013$). In a separate experiment that was not inhibitor based, an adenovirus was used to re-introduce wild type or mutant PTEN into PTEN-null M43 cells. Phospho-AKT levels were diminished and there was disrupted cell cycle progression in cells infected with wild-type PTEN, but not in cells infected with mutant PTEN (data not shown).

To determine if inhibition of PI3K/AKT signaling increases the sensitivity of MM cells to a standard chemotherapeutic agent, we treated serum-starved M43 cells with LY294002, cisplatin, or a combination of LY294002 and cisplatin (Figure 6a, left panel). Importantly, the combination of LY294002 and cisplatin resulted in enhanced inhibition of cell proliferation as compared to treatment with either agent alone ($P<0.0001$). The same conditions were used to treat a second cell line, M17, which has lower AKT activity than M43 under serum-starvation conditions. Despite having comparatively low AKT activity and being relatively insensitive to LY294002, in M17 cells the combination of LY294002 and cisplatin still decreased cell proliferation with greater efficacy than either drug alone ($P=0.0006$) (Figure 6a, right panel). Compared to single agents, treatment with a combination of

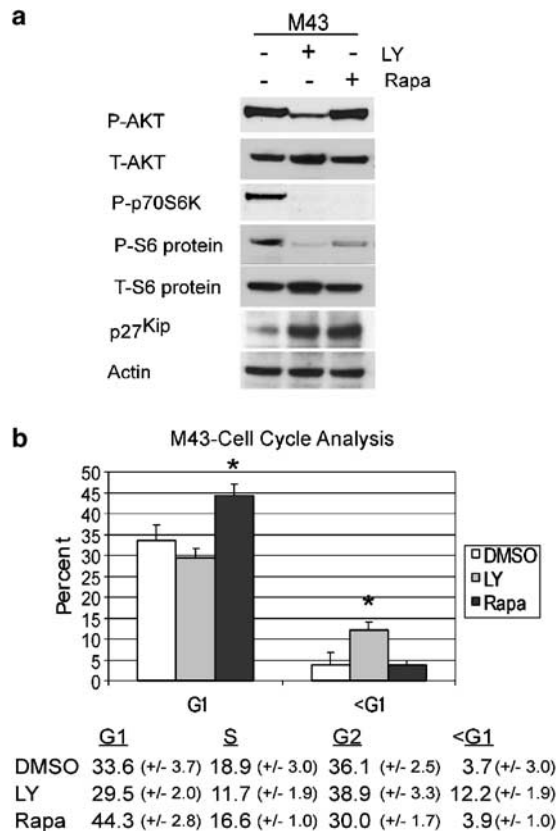


Figure 5 MM cells with high basal AKT activity are sensitive to targeted disruption of AKT signaling. (a) M43 cells treated with 20 μ M LY294002 or 100 ng/ml rapamycin for 48 h. Right, representative Western blot showing downregulation of AKT phosphorylation in response to LY294002. Inhibition of mTOR signaling in both LY294002- and rapamycin-treated cells is shown by loss of phosphorylated p70S6K and downstream S6 protein. p27^{Kip} expression, indicative of cell cycle arrest, is increased in response to both inhibitors. (b) Representative flow cytometry results depicting a 30% increase in the average percent of cells in G1 phase following rapamycin treatment, whereas LY294002 treatment resulted in a 3.3-fold increase in the population of cells in the <G1 phase, indicative of cell death. Error bars are indicative of standard deviation. Asterisks (*) represent a statistically significant increase in the number of cells in G1 or sub-G1 compared to DMSO control. Table showing the average percentage of cells in each phase of the cell cycle in placebo (DMSO), rapamycin (Rapa) and LY294002 (LY)-treated M43 cells

LY294002 and cisplatin inhibited cell proliferation by 2.4-fold in M43 cells and 1.4-fold in M17 cells.

We further tested the ability of LY294002 and cisplatin to induce apoptosis in M43 cells. Two independent assays for cleaved PARP (Figure 6b, left) and DNA fragmentation (Figure 6b, right) showed that the combination of LY294002 and cisplatin was more effective at inducing apoptosis than single agents alone. Collectively, these results suggest that targeted disruption of AKT activity sensitizes MM cells to conventional chemotherapeutic agents such as cisplatin, and that sensitivity to AKT inhibition may be more effective in MM cells having elevated AKT activity.

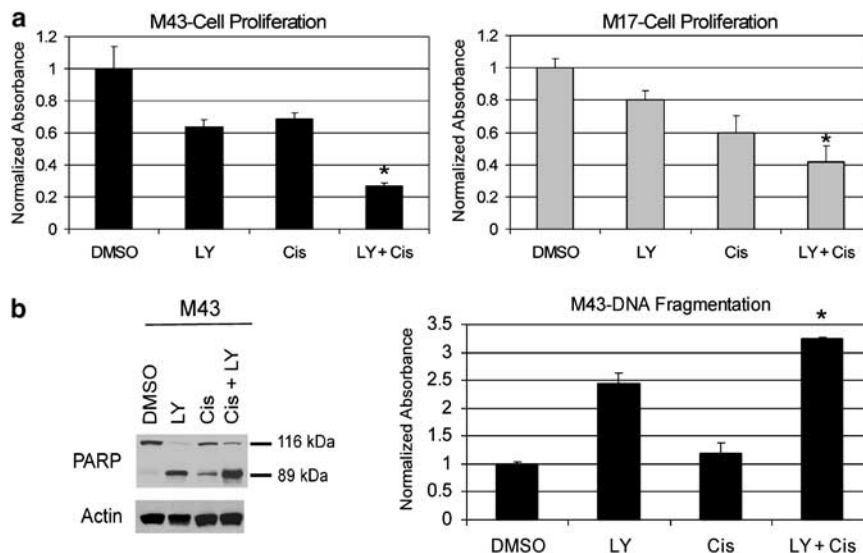


Figure 6 Inhibition of AKT activity in M43 cells contributes to cell death. **(a)** Targeted disruption of upstream PI3K with LY294002 inhibits the growth of MM cells. Cell proliferation assay of MM cells after 48 h of treatment with 10 μ M LY294002 (LY), 20 μ M cisplatin (Cis) or a combination of LY + Cis. Absorbance values were normalized to DMSO-treated controls. Asterisks (*) represent statistically significant enhanced inhibition of cell proliferation in LY + Cis-treated cells compared to DMSO, LY- or Cis-treated cells. Note that M43 cells with high basal AKT activity had greater sensitivity to LY compared to M17 cells with lower basal AKT activity. A greater effect on cell proliferation was observed in M43 cells treated with LY + Cis than in M17 cells treated with the same combination of drugs. **(b)** Inhibition of PI3K in M43 cells increases cisplatin-induced apoptosis. Right, Western blot of M43 cells showing that the 89-kDa PARP cleavage marker of apoptosis is increased in LY + Cis-treated cells compared to DMSO-, LY- or Cis-treated cells. Left, DNA fragmentation detected using a Cell Death Detection ELISA Kit (Roche Diagnostics). Values were normalized to DMSO-treated controls. Asterisks (*) represent statistically significant (Student's *t*-test, $P < 0.05$) enhanced DNA fragmentation in LY + Cis-treated cells compared to DMSO, LY- or Cis-treated cells

Discussion

MM is a highly aggressive form of cancer, and there currently are no effective therapies for this disease (Rusch, 2003). In particular, there is an insufficient understanding of the apoptosis-resistant phenotype of MM.

It is now evident that AKT is a central player in a signaling pathway of which many components have been linked to tumorigenesis. Upstream PI3K (Shayesteh *et al.*, 1999; Philp *et al.*, 2001; Samuels *et al.*, 2004), PTEN (reviewed in Di Cristofano and Pandolfi, 2000) and LKB1 (Boudeau *et al.*, 2003), and downstream tuberous sclerosis complex 2 (TSC2) (reviewed in Kwiatkowski, 2003; Manning and Cantley, 2003) and eIF4E (Avdulov *et al.*, 2004; Bjornsti and Houghton, 2004; Mamane *et al.*, 2004; Wendel *et al.*, 2004) have each been implicated in cancer biology. Collectively, these signaling proteins contribute to the PI3K/AKT/mTOR signaling cascade that, when deregulated, leads to disrupted translation of mRNAs that are involved in processes such as cell cycle progression, growth stimulation, cell survival, invasion and interaction with the extracellular matrix (Mamane *et al.*, 2004).

Here we show that the AKT/mTOR pathway is frequently activated in both human and murine MM specimens and MM cell lines. Immunohistochemical analysis revealed elevated levels of phospho-AKT in nearly two-thirds of human MM tumors. A strong

association with elevated phospho-mTOR positivity in these same tumors confirmed activation of the AKT pathway.

In tumor cells, AKT can be activated by a variety of mechanisms, including loss or downregulation of PTEN (Eng, 2003), mutation of the PI3K catalytic or regulatory subunits *PIK3CA* or *PIK3R*, respectively (Philp *et al.*, 2001; Samuels *et al.*, 2004), activation of PI3K due to autocrine or paracrine stimulation of receptor tyrosine kinases (Nakatani *et al.*, 1999; Yuan *et al.*, 2000; Tanno *et al.*, 2001; Eng, 2003), and/or Ras activation (Liu *et al.*, 1998). Although it was not the intention of this investigation to explore all of the possible mechanisms that might contribute to AKT activation in MM, we did document two mechanisms that can activate the AKT pathway in MM cells, that is, HGF stimulation and PTEN loss. In MM, as is the case in other tumor types, for example, lung and ovarian carcinomas (Brognard *et al.*, 2001; Altomare *et al.*, 2004), elevated AKT activity in tumor-derived cell lines is relatively infrequent under serum-starved conditions. In fact, our only MM cell line with elevated basal levels of AKT activity had loss of PTEN. The marked increase in AKT activity upon HGF stimulation, even in cells with high AKT activity, is consistent with our previous findings showing that tumor cells transfected with activated AKT are still responsive to growth factor stimulation (Tanno *et al.*, 2001). Although the levels of active AKT may be elevated further by exogenous

HGF, this may not be physiologically relevant *in vitro* since increased phosphorylation of downstream mTOR was not observed in HGF-stimulated M43 cells with high basal mTOR activity. In tumor tissues, however, paracrine growth factor stimulation may be a common mechanism by which the AKT pathway is stimulated. Germane to this, HGF and Met are often overexpressed in MM (Tolnay *et al.*, 1998), and HGF enhances the invasiveness of MM cells (Klominck *et al.*, 1998; Harvey *et al.*, 2000). Moreover, AKT has been shown to mediate antiapoptotic signaling by HGF/Met (Bowers *et al.*, 2000; Xiao *et al.*, 2001), and simian virus 40, which has been implicated in the pathogenesis of some human MMs (reviewed in Rizzo *et al.*, 2001), induces HGF/Met activation in mesothelial cells (Cacciotti *et al.*, 2001).

PTEN loss appears to be a relatively infrequent cause of AKT activation in MM. To our knowledge, this is the first report of a homologous deletion of the *PTEN* tumor suppressor gene in MM. A previous analysis of the *PTEN* gene in 18 primary MMs did not uncover any mutations (Papp *et al.*, 2001). In our series, however, loss of the *PTEN* gene was detected in one of nine human MM cell lines, and loss of PTEN protein expression was observed in two of 26 human MM specimens. Collectively, these data indicate that loss of functional PTEN, a negative regulator of the AKT pathway, occurs in less than 10% of MMs.

All of our human MM cell lines had at least some AKT activity under serum-deprivation conditions. Likewise, all of our murine MM lines had Akt activity under similar conditions. However, it is noteworthy that all five tumors from which these murine MM cell lines were derived exhibited high Akt activity *in vivo*, based on immunohistochemical staining. Thus, although the frequency of elevated AKT activity in human MM cell lines is low in the absence of serum, the collective data suggest that most human and murine MM tumors would respond to AKT pathway inhibition *in vivo*.

Rapamycin and its pharmaceutical analogs, CCI-779 and RAD001, are currently being tested for efficacy against a broad range of refractory tumors. An important challenge for clinical development is to better identify tumors that are likely to be sensitive to mTOR inhibition. *In vitro* data presented here suggest that pharmacologic inhibition of mTOR may have therapeutic efficacy in MM patients with aberrant AKT signaling, in agreement with studies of *Pten*-deficient mice showing that Akt activation is an important factor in predicting which tumors will be sensitive to mTOR inhibition (Neshat *et al.*, 2001; Podsypanina *et al.*, 2001).

It has been proposed that the extent of somatic genetic mutations present in a given tumor may influence sensitivity to rapamycin (Huang and Houghton, 2001). The marked therapeutic response observed in an Akt-dependent prostate intraepithelial neoplasia (PIN) model treated with RAD001 (Majumder *et al.*, 2003) raises the possibility that inhibitors

of mTOR may be effective in inducing a cytotoxic rather than a cytostatic response in early neoplastic lesions, which are likely to harbor few somatic genetic changes. However, the current clinical application of mTOR inhibition is targeted at later-stage cancers. Likewise, our study was confined to human MM cell lines having numerous chromosomal alterations typical of the disease, since cell lines from preneoplastic mesothelial lesions are not available.

The treatment of MM cells with rapamycin or LY294002 had different effects. Unlike the prostate PIN model (Majumder *et al.*, 2004), mTOR inhibition had no effect on MM cell death. At the 48-h timepoint selected for the cell cycle analysis, G1 arrest was evident for M43 cells treated with rapamycin, but an increased sub-G1 population indicative of apoptosis was already evident in M43 cells treated with LY294002. This does not rule out the possibility that rapamycin might induce more apoptosis after a prolonged time exposure. The different effect of LY294002 at inducing apoptosis may be attributed to its targeting of upstream PI3K and, therefore, directly inhibiting antiapoptotic pathways. Increased G1 arrest of LY294002-treated M43 cells was not observed because of increased cell death. Moreover, LY294002 augmented the chemotherapeutic sensitivity of MM cells to cisplatin. These data are consistent with findings in other tumor cell types showing that inhibition of PI3K/AKT signaling increases the efficacy of chemotherapeutic agents, such as paclitaxel and cisplatin (Brognard *et al.*, 2001; Hu *et al.*, 2002; Altomare *et al.*, 2004).

Treatment of MM cells with the PI3K inhibitor LY294002 enhanced the growth inhibitory effects of cisplatin. The degree to which combined LY294002 and standard chemotherapeutic drugs affects MM cell growth depends in part on the level of AKT activity in a given cell line. Thus, we noted that the combination of LY294002 and cisplatin had greater efficacy in M43 cells, which have relatively high constitutive AKT activity, than in M17 cells, which have lower AKT activity. These *in vitro* experiments provide a rationale for targeting AKT activity in MM patients to improve response to conventional chemotherapies. Such an improvement could have significant implications in MM, a very aggressive cancer for which response rates to either single-agent or combination chemotherapy have been historically low (Rusch, 2003).

Although M43 MM cells have not been tested for tumorigenicity in mice, we have observed elevated Akt activity in several other *in vivo* models of MM. These models present potential opportunities for future pre-clinical investigations to test the *in vivo* effects of AKT pathway inhibition on MM progression. Such studies would clarify further, in an *in vivo* MM model, whether AKT inhibition, either alone or in combination with standard chemotherapeutic agents, preferentially kills tumor cells that have a dependence on AKT activity for survival not shared by normal cells (Brognard *et al.*, 2001; West *et al.*, 2002).

Materials and methods

Immunohistochemistry

Slides containing sections of a human MM tumor tissue microarray (TMA) were obtained from the Biosample and Tissue Procurement Core Facility at Fox Chase Cancer Center (Philadelphia, PA, USA). The TMA contained tissue cores from two different regions of each of 19 tumor specimens from primary MM patients. Cores from normal tissue (lung, colon, and kidney) were used as negative controls. Additional slides from seven MM tumor patients were obtained from the Cooperative Human Tissue Network. Mouse tissues/tumors were obtained from asbestos-treated MM models (see below).

Slides containing formalin-fixed, paraffin-embedded samples were deparaffinized, hydrated in water and subjected to antigen retrieval in 10 mM citrate buffer, pH 6.0. Preparations were incubated in 3% H₂O₂ for 20 min, washed with H₂O or PBS, and blocked with 10% serum for 30 min. Phospho-AKT Ser473, phospho-mTOR Ser 2448 (Cell Signaling Technology, Beverly, MA, USA), Met and PTEN (Santa Cruz Biotechnology, Santa Cruz, CA, USA) antibodies were detected with biotinylated secondary antibodies. Negative controls were incubated with primary antibody preabsorbed with blocking peptide (Cell Signaling Technology). Tissue sections were stained with DAB chromagen and counterstained with hematoxylin. Surrounding non-neoplastic stroma and/or normal tissues served as internal negative controls for each slide. The slides were scored semiquantitatively. A score of 0 indicated no staining, 0.5 (+/–) was probably negative with some focal staining, 1 (+) was indicative of weak positivity with focal staining, 2 (++) indicated clearly positive staining, and a score of 3 (+++) was very positive. A score of 2 was indicative of elevated P-AKT or P-mTOR staining. To count a tumor as having elevated phospho-AKT or phospho-mTOR on the TMA, at least one of the two cores corresponding to an arrayed tumor must have scored ++ or +++.

In vivo models of MM

Mice were housed and treated according to guidelines established by the National Institutes of Health *Guide for the Care and Use of Laboratory Animals*.

For asbestos-induced MM, male wild-type mice derived from an inbred 129/Sv or mixed C57Bl/6 background, aged 6–8 weeks, were injected intraperitoneally with 400 µg of crocidolite (UICC grade; SPI Supplies, West Chester, PA, USA) in PBS every 21 days for a total of eight rounds of injections (total = 3.2 mg crocidolite per mouse). Disposable syringes (Becton Dickinson 3 ml Luer Lok syringe, 21 gauge needle) were filled with 1 ml of solution for intraperitoneal injections. Mice were killed by CO₂ asphyxiation upon detection of ascites, significant weight gain/loss or visible signs of distress. Ascites was aspirated off, and the intraperitoneal cavity was washed with sterile PBS. Collected cells were pelleted and resuspended in DMEM with 20% FBS to establish cell lines. Mouse tissues were fixed in 10% neutral buffered formalin and paraffin embedded for sectioning.

The murine MM cell line 40L is a highly-invasive, metastatic subline derived from a MM cell line isolated from a peritoneal explant of a male C57Bl/6 mouse that had received 50 weekly intraperitoneal injections of crocidolite asbestos fibers (Goodglick *et al.*, 1997). Metastatic tumors were established in syngeneic mice 1 month after intraperitoneal injection of 2 × 10⁶ cells suspended in 1 ml of PBS.

For the xenografts established from the human REN MM cell line (a gift from Dr S Albelda, University of Pennsylvania,

Philadelphia, PA, USA), 5 × 10⁶ cells suspended in 1 ml of PBS were injected intraperitoneally in male NOD/SCID mice. Locally invasive tumors were reproducibly established after one month.

Cell culture

Human MM cell lines were established from surgically explanted primary tumors as described previously (Taguchi *et al.*, 1993) and grown in RPMI 1640 with 10% FBS, supplemented with L-glutamine and penicillin/streptomycin. Mouse MM cell lines were derived from asbestos-treated mice, as described above, and grown in DMEM with 10% FBS.

For HGF stimulation, MM cell lines were serum starved overnight and treated with 10 U/ml HGF (a gift from Dr GF Vande Woude) for 10–20 min prior to harvesting cells. Alternatively, 50 ng/ml IGF-1 was used to stimulate MM cell lines for 20 min prior to harvesting. For experiments involving insulin, cells were serum-starved for 18 h and then stimulated with 100 nM insulin for 15 min prior to harvesting. For inhibition of the AKT signaling pathway, cells were treated with either 20 µM LY294002 (Calbiochem, La Jolla, CA, USA) or 100 ng/ml rapamycin (Sigma, St Louis, MO, USA) for 24–48 h under serum deprivation.

Western blot and immunoprecipitation analysis

Tissue samples were homogenized in lysis buffer (50 mM Tris-HCl (pH 7.5), 137 mM NaCl, 1 mM EDTA, 1% Nonidet P-40, 0.2% Triton X-100, 10% glycerol, 0.1 mM sodium orthovanadate, 10 mM sodium pyrophosphate, 20 mM β-glycerophosphate, 50 mM NaF, 1 mM phenylmethylsulfonyl fluoride, 2 µM leupeptin, and 2 µg/ml aprotinin). Insoluble material was removed by centrifugation at 4°C for 15 min at 18400 g. Protein concentration was determined with a BioRad Protein Assay Kit (BioRad Laboratories, Hercules, CA, USA).

Actin expression was used as a control to assess protein extract quality. For detection of protein expression, 20–30 µg of protein was subjected to Western blot analysis. Membranes were blocked and incubated with primary antibodies for 1 h in Tris-buffered saline containing 1% nonfat dry milk/0.1% Tween-20. Primary antibodies included: actin, PTEN, AKT1/2, Met, PARP (Santa Cruz Biotechnology, Santa Cruz, CA, USA), phospho-AKT Ser473, phospho-mTOR Ser2448, phospho-p70S6 kinase Thr389, phospho-S6 protein Ser 235/236, total S6-protein, total 4E-BP1, caspase 3 (Cell Signaling Technology, Beverly, MA, USA) and p27^{Kip1} (Transduction Laboratories, Lexington, KY, USA). Detection of antigen-bound antibody was carried out with the Renaissance Chemiluminescence Reagent Plus system (NEN Life Science, Boston, MA, USA).

For detection of PTEN expression, 200 µg of protein from cell lysates was immunoprecipitated with anti-PTEN (N-19, Santa Cruz Biotechnology, Santa Cruz, CA, USA) antibodies, following incubation with protein A:protein G agarose beads. Immunoprecipitates were subjected to 7.5% SDS-PAGE followed by immunoblotting. Alternately, PTEN expression was detected by direct Western blot detection using anti-PTEN antibody from Cell Signaling Technology.

In vitro AKT kinase assay

Protein extract (300 µg) was incubated with 2 µg of anti-AKT2 antibody (Upstate Biotechnology, Waltham, MA, USA), and the immunocomplex was precipitated with protein A:protein G (1:1) agarose beads (Life Technologies, Gaithersburg, MD, USA) at 4°C overnight. Immunoprecipitates were incubated with 5 µM [γ -³²P]ATP in kinase buffer (20 mM HEPES (pH 7.4),

10 mM MgCl₂, 10 mM MnCl₂) at 30°C for 25 min using histone H2B as substrate. The reactions were terminated by the addition of 2 × Laemml sample loading buffer and then subjected to 15% SDS-PAGE. Phosphorylation of histone H2B was visualized by autoradiography and quantitated with a BAS-1000 phosphorimager (Fuji Medical Systems, Stamford, CT, USA).

SSCP analysis

PCR was performed in a final volume of 10 μl with 30 ng of genomic DNA, 150 ng of each primer, 50 μM of each dNTP, 1.2 U of *AmpliTag* DNA polymerase (Perkin Elmer, Branchburg, NJ, USA) and 0.2 μCi [α -³²P]dCTP (DuPont NEN, Wilmington, DE, USA), using an MJ Research PTC-100 programmable thermal controller (MJ Research, Inc., Waltham, MA, USA). Primers were designed to amplify the complete sequences of exons 2–9 of the *PTEN* gene. Specifically for Figure 5b, primers to amplify a 256-bp genomic fragment encompassing exon 2 were 5' TCAGAT ATTTCTTTCCTT-AACTAAAGT 3' and 5' AAAAAATG ATTATAGAGCACTACAA-TA 3'. Primers to amplify a 296-bp genomic fragment corresponding to the amino terminal end of exon 8 were 5' AGGTGAAGATTTCTTTTTTA 3' and 5' TTCGGTTGGCTTTGTCTTTA 3'. Amplification conditions consisted of an initial denaturation of 5 min at 94°C followed by 20 cycles of 30 s at 94°C, 1 min at 64–54°C (with –0.5°C every cycle) and 1 min at 72°C, then 10 cycles of 30 s at 94°C, 30 s at 54°C, and 30 s at 72°C, and a final extension of 5 min at 72°C. PCR products were diluted 1:10 with 10 μM NaOH/20 mM EDTA gel-loading buffer, heat denatured at 94°C for 5 min and chilled on ice. A measure of 3 μl of each PCR product were separated electrophoretically on a 0.6 × denaturing gel. Gels were electrophoresed at 6 W of constant power for 12–18 h at room temperature, dried at 80°C under vacuum, and exposed to X-ray film.

PCR analysis of *PTEN*

For PCR amplification, 100 ng of genomic DNA was amplified in a 50 μl reaction using the following primers. In addition to the primers for exon 2 that were used for the SSCP analysis of *PTEN* (exon 2 (a)), new primers were synthesized to amplify a 297 bp-fragment for control *GAPDH* (5' GCGAGATCCCTC CAAAATCA 3' and 5' CTGATGATCTTGAGGCTGTG 3'), an alternate 210 bp-fragment for exon 2 (exon 2 (b), 5' CTAAAGTACTCAGATATTTATCC 3' and 5' AATAGTTT ACATCACAAAGTATCT 3'), a 347 bp-fragment corresponding to exon 1 (5' TTCGGAGGATTATTCGTC-TC 3' and 5' AGGTCAAGTCTAAGTCGA-TC 3'), and a 140 bp-fragment corresponding to exon 3 (5' CATTTGTTAATGGTG GCTTTTTG 3' and 5' CTCAATATTGTTTTAGAAGAT ATT 3'). Reactions were run side-by-side in a thermal cycler. Amplification conditions consisted of an initial denaturation of 4 min at 94°C followed by 37 cycles of 1 min at 94°C, 1 min

at 52°C and 1 min at 72°C, then one cycle of 1 min at 94°C, 1 min at 52°C, and 2 min at 72°C. PCR products were separated on a 2% agarose gel and visualized with ethidium bromide.

Cell cycle arrest analysis

Cells were harvested by trypsinization, washed and then fixed in 70% ethanol at –20°C. Cells were washed and stained with 10 μg/ml propidium iodide (Sigma, St Louis, MO, USA) in the presence of 100 μg/ml DNase-free RNase (Sigma). After 30 min at 37°C, cells were analysed by a fluorescent activated cell sorter (FACS) can (Becton Dickinson, San Jose, CA, USA) using Cell Quest software (Becton Dickinson).

Cell proliferation assays

Cell proliferation was measured with a CellTiter 96 (Promega, Madison, WI, USA) colorimetric assay, utilizing an MTS tetrazolium compound, as per the manufacturer's instructions. MM cells with similar sensitivities to LY294002 and cisplatin were used. In brief, MM cells were plated in 96-well microtiter plates at a concentration of 6.5 × 10³ cells per well and incubated overnight in RPMI medium containing 10% serum. Medium was aspirated and replaced with RPMI (no serum) containing inhibitor or placebo (DMSO). Inhibitor treatments were as follows: 10–20 μM LY294002 alone, 5–20 μM cisplatin (Cis, Calbiochem) alone, and a combination of 10–20 μM LY294002 for 2 h followed by the addition of 5–20 μM cisplatin. Cell viability was assessed at 24 and 48 h.

DNA fragmentation assay

Cells were treated with 10–20 μM LY294002 and/or 10–20 μM cisplatin for 24–48 h. Cells were lysed using lysis buffer provided in the Cell Death Detection ELISA kit (Roche Molecular Biochemicals). Apoptosis was determined by measuring DNA fragmentation following the manufacturer's instructions.

Acknowledgements

CA-45745, CA-77429, and CA-06927 from the National Cancer Institute, appropriation from the Commonwealth of Pennsylvania, and the Local No. 14 Mesothelioma Fund of the International Association of Heat and Frost Insulators & Asbestos Workers in memory of Hank Vaughan and Alice Haas awarded to JRT; ES-003721 from the National Institute of Environmental Health Sciences awarded to ABK. The following Fox Chase Cancer Center shared facilities were used in the course of this work: Cell Culture, Flow Cytometry and Cell Sorting, Biostatistics, Biochemistry and Biotechnology, Tumor Bank and Histopathology Facilities. We also thank ER Guh, a Howard Hughes Medical Institute Student Scientist, for technical assistance.

References

- Altomare DA, Wang HQ, Skele KL, De Rienzo A, Klein-Szanto AJ, Godwin AK and Testa JR. (2004). *Oncogene*, **23**, 5853–5857.
- Avdulov S, Li S, Michalek V, Burchrichter D, Peterson M, Perlman DM, Manivel JC, Sonenberg N, Yee D, Bitterman PB and Polunovsky VA. (2004). *Cancer Cell*, **5**, 553–563.
- Bellacosa A, Kumar C, Di Cristofano A and Testa JR. *Adv. Cancer Res.* in press.
- Bjornsti MA and Houghton PJ. (2004). *Cancer Cell*, **5**, 519–523.
- Boudeau J, Sapkota G and Alessi DR. (2003). *FEBS Lett.*, **546**, 159–165.
- Bowers DC, Fan S, Walter KA, Abounader R, Williams JA, Rosen EM and Lattera J. (2000). *Cancer Res.*, **60**, 4277–4283.
- Britton M. (2002). *Semin. Oncol.*, **29**, 18–25.

- Brognard J, Clark AS, Ni Y and Dennis PA. (2001). *Cancer Res.*, **61**, 3986–3997.
- Cacciotti P, Libener R, Betta P, Martini F, Porta C, Procopio A, Strizzi L, Penengo L, Tognon M, Mutti L and Gaudino G. (2001). *Proc. Natl. Acad. Sci. USA*, **98**, 12032–12037.
- Cao XX, Mohuiddin I, Ece F, McConkey DJ and Smythe WR. (2001). *Am. J. Respir. Cell Mol. Biol.*, **25**, 562–568.
- Craighead JE and Mossman BT. (1982). *New Engl. J. Med.*, **306**, 1446–1455.
- Di Cristofano A and Pandolfi PP. (2000). *Cell*, **100**, 387–390.
- Eng C. (2003). *Hum. Mutat.*, **22**, 183–198.
- Goodglick LA, Vaslet CA, Messier NJ and Kane AB. (1997). *Toxicol. Pathol.*, **25**, 565–573.
- Harvey P, Clark IM, Jaurand MC, Warn RM and Edwards DR. (2000). *Br. J. Cancer*, **83**, 1147–1153.
- Hu L, Hofmann J, Lu Y, Mills GB and Jaffe RB. (2002). *Cancer Res.*, **62**, 1087–1092.
- Huang S and Houghton PJ. (2001). *Drug Resistance Updates*, **4**, 378–391.
- Klominek J, Baskin B, Liu Z and Hauzenberger D. (1998). *Int. J. Cancer*, **76**, 240–249.
- Kwiatkowski DJ. (2003). *Ann. Hum. Genet.*, **67**, 87–96.
- Liu AX, Testa JR, Hamilton TC, Jove R, Nicosia SV and Cheng JQ. (1998). *Cancer Res.*, **58**, 2973–2977.
- Majumder PK, Febbo PG, Bikoff R, Berger R, Xue Q, McMahon LM, Manola J, Brugarolas J, McDonnell TJ, Golub TR, Loda M, Lane HA and Sellers WR. (2004). *Nat. Med.*, **10**, 594–601.
- Majumder PK, Yeh JJ, George DJ, Febbo PG, Kum J, Xue Q, Bikoff R, Ma H, Kantoff PW, Golub TR, Loda M and Sellers WR. (2003). *Proc. Natl. Acad. Sci. USA*, **100**, 7841–7846.
- Mamane Y, Petroulakis E, Rong L, Yoshida K, Ler LW and Sonenberg N. (2004). *Oncogene*, **23**, 3172–3179.
- Manning BD and Cantley LC. (2003). *Trends Biochem. Sci.*, **28**, 573–576.
- Nakatani K, Thompson D, Barthel A, Sakaue H, Liu W, Weigel RJ and Roth RA. (1999). *J. Biol. Chem.*, **274**, 21528–21532.
- Neshat MS, Mellinghoff IK, Tran C, Stiles B, Thomas G, Petersen R, Frost P, Gibbons JJ, Wu H and Sawyers CL. (2001). *Proc. Natl. Acad. Sci. USA*, **98**, 10031–10033.
- Nowak AK, Lake RA, Kindler HL and Robinson BW. (2002). *Semin. Oncol.*, **29**, 82–96.
- Papp T, Schipper H, Pemsel H, Unverricht M, Muller KM, Wiethage T, Schiffmann D and Rahman Q. (2001). *Oncol. Rep.*, **8**, 1375–1379.
- Philp AJ, Campbell IG, Leet C, Vincan E, Rockman SP, Whitehead RH, Thomas RJ and Phillips WA. (2001). *Cancer Res.*, **61**, 7426–7429.
- Podsypanina K, Lee RT, Politis C, Hennessy I, Crane A, Puc J, Neshat M, Wang H, Yang L, Gibbons J, Frost P, Dreisbach V, Blenis J, Giacong Z, Fisher P, Sawyers C, Hedrick-Ellenson L and Parsons R. (2001). *Proc. Natl. Acad. Sci. USA*, **98**, 10320–10325.
- Pullen N and Thomas G. (1997). *FEBS Lett.*, **410**, 78–82.
- Rizzo P, Bocchetta M, Powers A, Foddis R, Stekala E, Pass HI and Carbone M. (2001). *Semin. Cancer Biol.*, **11**, 63–71.
- Rusch VW. (2003). *J. Clin. Oncol.*, **21**, 2629–2630.
- Samuels Y, Wang Z, Bardelli A, Silliman N, Ptak J, Szabo S, Yan H, Gazdar A, Powell SM, Riggins GJ, Willson JK, Markowitz S, Kinzler KW, Vogelstein B and Velculescu VE. (2004). *Science*, **304**, 554.
- Shayesteh L, Lu Y, Kuo WL, Baldocchi R, Godfrey T, Collins C, Pinkel D, Powell B, Mills GB and Gray JW. (1999). *Nat. Genet.*, **21**, 99–102.
- Sonenberg N and Gingras AC. (1998). *Curr. Opin. Cell Biol.*, **10**, 268–275.
- Taguchi T, Jhanwar SC, Siegfried JM, Keller SM and Testa JR. (1993). *Cancer Res.*, **53**, 4349–4355.
- Tanno S, Tanno S, Mitsuuchi Y, Altomare DA, Xiao GH and Testa JR. (2001). *Cancer Res.*, **61**, 589–593.
- Tolnay E, Kuhnen C, Wiethage T, Konig JE, Voss B and Muller KM. (1998). *J. Cancer Res. Clin. Oncol.*, **124**, 291–296.
- Vogelzang NJ, Rusthoven JJ, Symanowski J, Denham C, Kaukel E, Ruffie P, Gatzemeier U, Boyer M, Emri S, Manegold C, Niyikiza C and Paoletti P. (2003). *J. Clin. Oncol.*, **21**, 2636–2644.
- Wendel HG, De Stanchina E, Fridman JS, Malina A, Ray S, Kogan S, Cordon-Cardo C, Pelletier J and Lowe SW. (2004). *Nature*, **428**, 332–337.
- West KA, Sianna Castillo S and Dennis PA. (2002). *Drug Resistance Updates*, **5**, 234–248.
- Wu H, Goel V and Haluska FG. (2003). *Oncogene*, **22**, 3113–3122.
- Xiao GH, Jeffers M, Bellacosa A, Mitsuuchi Y, Vande Woude GF and Testa JR. (2001). *Proc. Natl. Acad. Sci. USA*, **98**, 247–252.
- Yuan ZQ, Sun M, Feldman RI, Wang G, Ma X, Jiang C, Coppola D, Nicosia SV and Cheng JQ. (2000). *Oncogene*, **19**, 2324–2330.